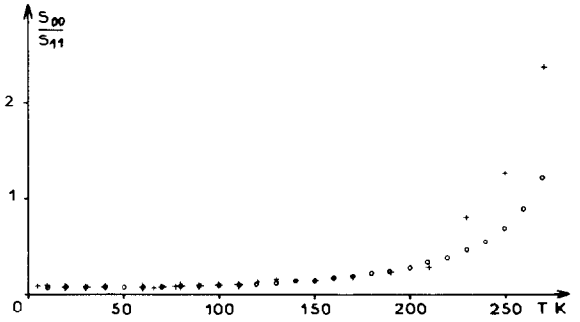

Fig. 2. Comparison between the temperature dependences of the ratio S_{oo}/S_{11} of the integrated intensities of the $^5D_o \rightarrow {}^7F_o$ emission to the $^5D_1 \rightarrow {}^7F_1$ one in the spectra recorded under pulsed selective excitation into the $^5D_1$ level (o) and continuous ultraviolet excitation (+).

ficantly to the optical properties of the Sm^{2+}: BaClF system at temperatures up to 300 K [4–6]. The physical explanation for these discrepancies lies in the fact that the feeding of levels ^5D_o and $^5D_1$ during the excitation pulse depends strongly on the pumping conditions [1]. Obviously, the role of the $^5D_o \rightarrow {}^5D_1$ radiationless transition will be enhanced if the population of the ^5D_o state at the end of the pulse is significant, as is the case for the ^5D_o pumping. On the other hand, the contribution of this transition will be reduced if the ^5D_o population remains equal to zero during the excitation pulse, as is the case for the $^5D_1$ or $^5D_2$ pumping. Under ultraviolet excitation, the feeding of the ^5D_o state during the pulse is ensured by fast non radiative processes connecting the $4f^5$-5d states directly to the ^5D_o state at temperatures above 200 K as it clearly appears from the comparison between the temperature dependences of the ratio S_{oo}/S_{11} of the integrated intensities of the $^5D_o/{}^7F_o$ emission to the $^5D_1 \rightarrow {}^7F_1$ one in the spectra recorded under selective excitation into the $^5D_1$ level on one hand, and ultraviolet excitation on the other hand (Fig. 2).

Thus, the thermalization near room temperature between two rare-earth levels separated by an energy gap of several times the maximum phonon frequency in the crystal (294 cm^{-1} in BaClF) [6] may be observed or not, depending on the optical pumping frequency. Similar investigations in other rare-earth systems such as Eu^{3+} doped materials, with larger $^5D_1 - {}^5D_o$ gaps and higher $4f^5$-5d state energies should be of interest to complement this observation.

1 J. G. Gâcon, M. F. Joubert, M. Blanchard and B. Jacquier, *Phys. Rev., (to appear)*.
2 A. S. M. Mahbub'ul Alam and Baldassare di Bartolo, *Phys. Rev. Letters, 19*, 1030 (1967).
3 A. S. M. Mahbub'ul Alam and Baldassare di Bartolo, *J. Chem. Phys., 47*, 3790 (1967).
4 J. C. Gâcon, J. C. Souillat, J. Sériot and B. di Bartolo, *Phys. Status Solidi A39*, 147 (1977).
5 F. Gaume, J. C. Gâcon, J. C. Souillat, J. Sériot and B. di Bartolo, in 'The Rare-Earths in Modern Science and Technology', Plenum, New York, 1978.
6 J. C. Gâcon, 'State Doctorate Thesis', Lyons University, *unpublished* (1978).

B18

Mechanisms for f–f Transition Probabilities in Lanthanide Coordination Compounds

S. F. MASON

Chemistry Department, King's College, London WC2R 2LS, U.K.

The Laporte-forbidden transitions of Ln(III) coordination compounds acquire a first-order electric-dipole probability from transient dipoles induced in the ligand groups by an allowed even-multipole electric moment of the f–f excitation, and by the mixing of the f–f with f–d and f–g electron promotions under the electrostatic field of the ligands. Applied initially to Ln(III) complexes containing monoatomic ligands which have an effective isotropic polarizability the ligand-polarization mechanism is found to depend, on extension to the corresponding polyatomic ligand cases, upon the anisotropy of the ligand polarizability tensor in complexes belonging to the higher non-centric symmetries. The electrostatic field and the ligand polarization mechanisms make complementary intensity contributions to the f–f transitions of a given Ln(III) complex type, dependent upon the rank of the leading electric multipole moment. The polarization mechanism contributes principally to the intensities of the ligand-hypersensitive 2^2-pole f–f transitions, whereas the electrostatic mechanism is predominant for the 2^6-pole transition intensities, and makes the more important contribution in the 2^4-pole cases.

B19

Absorption and Fluorescence Spectra of Europium-(III) Compounds in Non-Aqueous Solutions

J. LEGENDZIEWICZ, W. STRĘK* and B. JEŻOWSKA-TRZEBIATOWSKA

Institute of Chemistry, University of Wrocław, Wrocław, Institute for Low Temperature and Structure Research, Polish Academy of Sciences, Wrocław, Poland

The absorption and fluorescence spectra of Eu(III) compounds were investigated at room temperature in different non-aqueous solutions.

It was found that the intensity of hypersensitive bands is closely related to the refractivity of solvent. A possible mechanism of solvent effect on intensities of f–f transition is discussed within the framework of the Mason's polarizability mechanism.

Effect of solvent on fluorescence properties of Eu(III) was investigated and mechanism of fluorescence quenching is proposed.

B20

Application of the Luminescence and Absorption Spectroscopy and the X-ray Method to the Study of Ln^{3+} Ions Interactions with Aminoacids

J. LEGENDZIEWICZ, E. HUSKOWSKA

Institute of Chemistry, University of Wrocław, Poland

G. ARGAY

Central Research Institute for Chemistry of Hungarian Academy of Sciences, Budapest, Hungary

and A. WAŚKOWSKA

Institute for Low Temperature and Structure Research Polish Academy of Sciences, Wrocław, Poland.

The Nd^{3+}, Ho^{3+} and Eu^{3+} complexes with glycine, alanine and glutamic acid were synthetized and obtained in a form of monocrystals. Absorption and luminescence spectra recorded in the region of 8000–35000 cm^{-1} were measured along the crystallographic axes. Intensities of the f–f transitions were analysed on the base of Judd theory. The X-ray crystal structure determination of the $Nd(gly)_3(ClO_4)_3 4 \cdot 5H_2O$ is reported. Crystals are triclinic, space group $P\bar{1}$, with a = 11.554(4) Å, b = 14.108(1) Å, c = 15.660(3) Å, α = 97.11(1)°, β = 102.82(2)°, γ = 105.20(2)°, V = 2355.25 Å^3, Z = 4, $M.W.$ = 747.7, D_c = 2.107 3 g cm^{-3}, D_m = 2.103 1 g cm^{-3}. The structure was solved by Patterson method and successive Fourier syntheses gave location of all non-hydrogen atoms. The final R factor was 0.062 and R_w = 0.073 for 12869 reflections with $|F_o| > 5\sigma|(F_o)|$. The coordination polyhedron of Nd atoms comprises of seven oxygen atoms from the glycine and two from water molecules. There are two types of Nd–gly contacts. The presence of oxygen bridges explains considerable difference in the Nd–Nd distances. There was stated the difference in the neodymium–glycine bonding mode in comparison with that observed for calcium–glycine complex.

B21

Derivatives of Hydrogen Uranyl Phosphate: Excited-state Properties of a Family of Lamellar Solids

ARTHUR B. ELLIS*, MICHAEL M. OLKEN and RICHARD N. BIAGIONI

Department of Chemistry, University of Wisconsin-Madison, 1101 University Avenue, Madison, Wis. 53706, U.S.A.

The excited-state properties of the layered compound hydrogen uranyl phosphate (HUP), $HUO_2PO_4 \cdot 4H_2O$, and of solids derived therefrom by intercalative ion-exchange reactions have been examined. The reactions exploited are given in eqn. (1)–(3).

$$HUO_2PO_4 + M^+ \longrightarrow MUO_2PO_4 + H^+ \quad (1)$$

M = K, Ag, NH_4, NC_5H_6 (pyridinium),

n-$C_4H_9NH_3$, n-$C_8H_{17}NH_3$

$$HUO_2PO_4 + \tfrac{1}{2}M^{2+} \longrightarrow M_{1/2}UO_2PO_4 + H^+ \quad (2)$$

M = Ca, Zn, Cu (~0.4 equivalents incorporated)

$$HUO_2PO_4 + 1/3\ M^{3+} \longrightarrow M_{1/3}UO_2PO_4 + H^+ \quad (3)$$

M = $Cr(urea)_6$, Eu (~0.07 equivalents incorporated)

The products of these reactions have all been characterized by elemental analysis, IR spectroscopy, and X-ray powder diffraction. The latter reveals that all of the compounds retain the lamellar structure of HUP and can be indexed in tetragonal symmetry, using c lattice values derived from 00l data and a lattice values of ~6.99 Å. Although the a values are roughly constant, the interlamellar spacings (distance from the middle of one layer to the middle of the adjacent layer) vary widely; typical values are 8.69, 9.01, 10.34 and 18.76 Å for HUP, NH_4UP, $Ca_{1/2}$UP, and n-$C_8H_{17}NH_3$UP, respectively.

All of the samples exhibit electronic absorption spectra characteristic of the UO_2^{2+} chromophore; for substituent cations possessing visible absorption bands, these transitions appear superimposed in each spectrum. Except for the n-$C_8H_{17}NH_3^+$, Ag^+, Cu^{2+}, and $Cr(urea)_6^{3+}$ salts, the samples all exhibit yellow-green emission characteristic of the UO_2^{2+} moiety when excited with blue or near-UV light at 295 K. Emission decay curves are exponential for all of the emissive solids and yield lifetimes, τ, ranging from ~1–450 μs. Samples having τ values of ~10^2–10^3 μs include HUP and the NH_4^+, pyridinium$^+$, K^+, Ca^{2+}, and Zn^{2+} derivatives. These solids also have radiative quantum efficiencies, ϕ_r, approaching unity at 295 K. Values of τ and ϕ_r have been used to calculate